CERN-PH-EP/2005-023

Proposal for an absolute luminosity determination in colliding beam experiments using vertex detection of beam-gas interactions

Massimiliano Ferro-Luzzi *

CERN, CH-1211 Genève 23, Switzerland

Abstract

We propose a method for determining the absolute luminosity in a colliding-beam experiment at circular accelerators by measuring vertices of beam-gas interaction to determine the beam shapes and overlap. This method can be applied (for example) at all Large Hadron Collider experiments without modification of their detectors.

Key words: Absolute luminosity, colliding beam experiments, vertex detection
PACS: 29.20.-c, 29.27.-a, 29.27.Fh

* Corresponding author.
Email address: Massimiliano.Ferro-Luzzi@cern.ch (Massimiliano Ferro-Luzzi).

1 Introduction

The ability to determine cross-sections in colliding-beam particle physics experiments at storage rings is of general interest. For instance, the Large Hadron Collider (LHC) at CERN will start operation in the year 2007 and various experiments (e.g. ATLAS [1] and CMS [2]) count on precise cross-section measurements to detect new phenomena due to physics beyond the Standard Model (SM) of particle physics. Typical examples [3] are the measurements of the $t\bar{t}$ production cross-section, the determination of Higgs boson properties and possible distinction between a SM Higgs and a Minimal Supersymmetric SM Higgs, or in general the measurement of New Physics parameters (e.g. Supersymmetry), if New Physics are observed at the LHC. For these examples, the required relative accuracy on the absolute luminosity lies in the range 1-5%.

There are various ways that have been used in the past to measure cross-sections. Two methods remove the luminosity dependence by comparison of two cross-sections:

A1. The first method * is based on measuring the inelastic cross-section and elastic cross-section at forward angle and eliminating the luminosity dependence [4] by a fundamental relation between these two cross-sections (optical theorem) [5].

A2. The second method is based on measuring the rates for a given 'reference' reaction of which the cross-section has either been precisely measured by other experiments or is claimed to be calculable with sufficient theoretical accuracy (e.g. the $pp \to pp\ell\ell$ process [6] or weak boson production [7] have been proposed for the LHC).

The two following methods measure *directly* the luminosity:

B1. The 'van der Meer scan' method [8]: one moves the beams transversely across each other and records the relative luminosity (reaction rate). The position for maximum luminosity is found and the absolute luminosity is inferred from the measured beam overlap and the beam currents. This method was successfully applied at the Intersecting Storage Rings at CERN. However, the conditions at the LHC will be drastically different (bunched beam versus coasting beams, similar horizontal and vertical beam sizes as opposed to widely different sizes, bunch-to-bunch variations, etc.).

B2. The 'wire method' which uses movable wires, scanned across the beams in the ring while recording reaction rates, in order to measure the beam

* Sometimes referred to in the literature as the 'luminosity-independent method', which is confusing since method A2 is also 'luminosity-independent'.

profiles [9]. Combined with a measurement of the total bunch charges, this method can give the absolute luminosity.

With the advent of precise microvertex detectors, an alternative way of measuring *directly* the absolute luminosity emerges. The purpose of this article is to describe this alternative method and its possible use at the LHC experiments (although it could be applied at other circular accelerators). The proposed method relies on beam-gas interactions for measuring the individual beam shapes and determining the beam overlap integral which enter the luminosity (see eq. 1 below). The method also allows measuring directly possible beam crossing angles or beam offsets.

The proposed method is non-destructive. Indeed, as will be shown, the target gas thickness required is much less than the integrated LHC residual gas density, and the induced radiation is not larger than the one caused by beam-beam collisions. This method should allow measuring the absolute luminosity individually for each colliding bunch pairs in a short time. We discuss how to measure in the same experiment the cross-section of any given reaction emerging from the colliding bunches (*pp* collisions). Once calibrated by this method, the chosen *pp* reaction (which could simply be e.g. the full 'visible' cross-section) can be used later to measure the absolute luminosity in a continuous way without the addition of target gas and *at any luminosity.*

The luminosity L for two counter-rotating bunches (labeled 1 and 2) with time- and position-dependent density functions $\rho_1(\mathbf{x},t)$ and $\rho_2(\mathbf{x},t)$ is given by [10]

$$L = f\, N_1\, N_2 \sqrt{(\mathbf{v}_1 - \mathbf{v}_2)^2 - \frac{(\mathbf{v}_1 \times \mathbf{v}_2)^2}{c^2}} \int \rho_1(\mathbf{x},t)\, \rho_2(\mathbf{x},t)\, d^3x\, dt \qquad (1)$$

for the case where the particles in each bunch are all moving with the same velocity $\mathbf{v}_1$ resp. $\mathbf{v}_2$ in the laboratory reference frame (more general formulas can be found in Ref. [11]). Here, we have defined f the revolution frequency and N_1 resp. N_2 the total number of protons in the bunches. The bunch particle densities $\rho_1(\mathbf{x},t)$ and $\rho_2(\mathbf{x},t)$ are normalized such that their individual integrals over full space are unity. If the two bunches are identical in shape (Gaussian) and perfectly overlapping with no crossing angle, then one obtains the more familiar relation

$$L = f \frac{N_1\, N_2}{4\pi\, \sigma_x\, \sigma_y} \qquad (2)$$

with $\sigma_{x,y}$ the variances of the two-dimensional Gaussian shape in the two transverse directions x and y. Corrections due to e.g. beam crossing angles and possible beam offsets are discussed later.

The method proposed here aims at measuring the densities ρ_1 and ρ_2 from beam-gas collisions. We assume the total number of protons in the bunches, N_1 and N_2, can be precisely measured by independent means.

This article is organized as follows. In section 2 we first give a rate estimate for beam-gas interactions, taking the LHC as an example application for the proposed method. We describe how to measure the beam profiles with beam-gas interaction vertices in section 3, where we consider the LHC and LHCb experiment [12] for illustration purposes. Some general features of beam-gas and beam-beam events at the LHC are discussed in section 4. Potential sources of systematic uncertainties are addressed in section 5. In section 6 we discuss some experimental aspects related to the gas target. Finally, a summary is given in section 7.

2 Rate estimate

We use the notation pp and pA to indicate beam-beam collisions ($\sqrt{s}$ = 14 TeV) and beam-gas collisions (with equivalent pp center-of-mass energy $\sqrt{s}$ = 114.5 GeV). We assume a constant density n of nuclei A and assume that the vertex detector allows reconstructing beam-gas interaction vertices over a distance d along z (assuming for simplicity a 'top hat' acceptance). Then, for a single circulating bunch, the rate R_{pA} of 'useful' bunch-gas interactions is

$$R_{pA} = a_{pA}\, \sigma_{pA}\, N\, f\, n\, d \ , \tag{3}$$

where N is the number of protons in the bunch and σ_{pA} the cross-section for pA collisions (essentially, the inelastic cross-section). The factor a_{pA}, which is typically of order unity (see below), accounts for the detector acceptance and for the definition of 'useful' events (which depends on the detailed data analysis). Note that the rate does not depend on the beam transverse size. We can assume for rough estimates that

$$\sigma_{pA} \approx \sigma_{p^1\mathrm{H}}\, A^{0.7} \tag{4}$$

where $\sigma_{p^1\mathrm{H}} \approx 40$ mb is the inelastic cross-section for p-^{1}H collisions at about 114.5 GeV center-of-mass energy (A is the atomic mass in amu).

To give a numerical example we consider the case of the LHC. We take Xe gas as target [†]. Therefore, assuming $A = 131$ (Xe), $N = 10^{11}$, $n = 2.5 \times 10^9$ cm^{-3}

[†] We choose xenon because of the large mass and because much of the LHC ring is coated with non-evaporable getter that may be too rapidly spoiled by exposure

(i.e. 10^{-7} mbar at 293 K), $d = 20$ cm and $a_{pA} = 0.4$, we obtain

$$R_{pA} \approx a_{pA}\, \sigma_{p^1\mathrm{H}}\, A^{0.7}\, N\, f\, n\, d \approx 30 \text{ Hz} . \tag{5}$$

If this bunch comes in collision with a similar bunch, then the rate R_{pp} of inelastic pp collisions is approximately given by

$$R_{pp} = a_{pp}\, f\, \sigma_{pp}\, \frac{N^2}{4\pi\, \sigma_x \sigma_y} \approx 1.4 \text{ kHz} , \tag{6}$$

where we have assumed $\sigma_{pp} \approx 80$ mb, $\sigma_x \approx \sigma_y \approx 200$ μm ($\beta^* \approx 34$ m) and $a_{pp} = 0.8$. The beam-gas rate would allow mapping the bunch profile within minutes with a statistical precision below 1%, while the simultaneously measured beam-beam rate would allow a precise determination of the 'visible' pp inelastic cross-section at 14 TeV.

Note that for the same conditions, assuming however that the gas density extends over a distance D ($\sim$ a few meters) of the LHC ring, the beam decay life time $\tau = (\sigma_{pA}\, n\, f\, D)^{-1}$ due to the target gas would be of the order of 1 year, well above the decay life time induced by the LHC residual gas (about 100 hours). Therefore, the proposed method can be considered non-disruptive for the LHC beams and for the accelerator.

3 Beam profile measurement

An essential prerequisite for the proposed method is the availability of a vertex detector which should be precise enough to allow mapping of the transverse beam shapes. In the case of LHCb, the primary vertex resolution for pp events that pass the trigger and produce a $b\bar{b}$ pair is about 10 μm in both x and y [12]. Comparable precisions are expected for the other major LHC experiments. However, this precision depends on the number of reconstructed tracks forming the vertex and may also depend on other variables such as the momentum [‡] or polar angle. For beam-gas interactions we expect a lower track multiplicity. We carried out a simple Monte-Carlo simulation using the event generator PYTHIA 6.205 [13] to compare beam-beam events and beam-gas events at the LHC. The resulting distributions of the number of charged particle [§] tracks per vertex, of their transverse momentum p_T and of their pseudo-

to non-noble gases. However, other target gases could be envisaged.

‡ For example, in LHCb the simulated impact parameter resolution varies roughly like 14 μm + 35 μm (GeV/c)/p_T [12], with p_T the transverse momentum.

§ More exactly, N_{tracks} is the sum of all $\mu^\pm$, $e^\pm$, $\pi^\pm$, $K^\pm$ and $p^\pm$ generated.

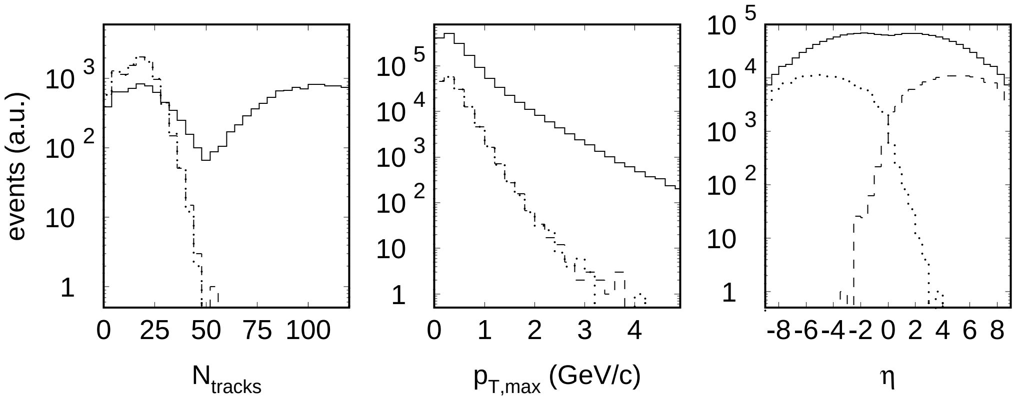

Fig. 1. Left: Number of charged particles emerging from beam-gas and beam-beam collisions. Middle: Transverse momentum distribution for charged particles. Right: pseudo-rapidity distributions for charged particles. In all cases: beam1-gas = dashed curve, beam2-gas = dotted curve, and beam-beam = solid curve.

rapidity ¶ η are shown in Fig. 1 for beam-gas ‖ and beam-beam events. We call 'beam 1' the LHC beam circulating clockwise when seen from above and 'beam 2' the counter-rotating beam. Note that the left and right bumps in the $N_{\rm tracks}$ distribution for beam-beam events are due to the contributions of 'soft' (diffractive, low-p_T) and 'hard' scattering events respectively. The separation between these two bumps is much less pronounced at the lower center-of-mass energy of beam-gas collisions.

To study the geometrical acceptance for beam-gas and beam-beam events at the LHC, and to investigate ways for distinguishing between the different types of interactions, we added a simplified geometry of the LHCb vertex detector (VELO) [14] to our Monte-Carlo simulation. In the following, we name 'reconstructable' tracks those charged particle tracks which traversed at least 4 tracking stations of the VELO in our Monte-Carlo simulation. The fraction of interactions (among all inelastic interactions) producing at least 6 reconstructable tracks is shown in Fig. 2 as a function of the primary vertex position along the beam axis ** z for the three types of events (beam1-gas, beam2-gas and beam-beam). Inelastic events were generated homogeneously over -1.2 m $< z <$ 1.2 m in all three cases. In the real experiment, beam-beam events will be weighed with a Gaussian-like distribution along z with an rms of about 53 mm.

¶ Defined as $\eta = -\ell n(\tan(\theta/2))$ with θ the polar angle.

‖ We mean here PYTHIA events with a 7 TeV beam and a fixed proton target. The track multiplicity might be somewhat larger for the actual proton-nucleus events.

** The interaction point is at $z = 0$ and beam 1 moves toward positive z.

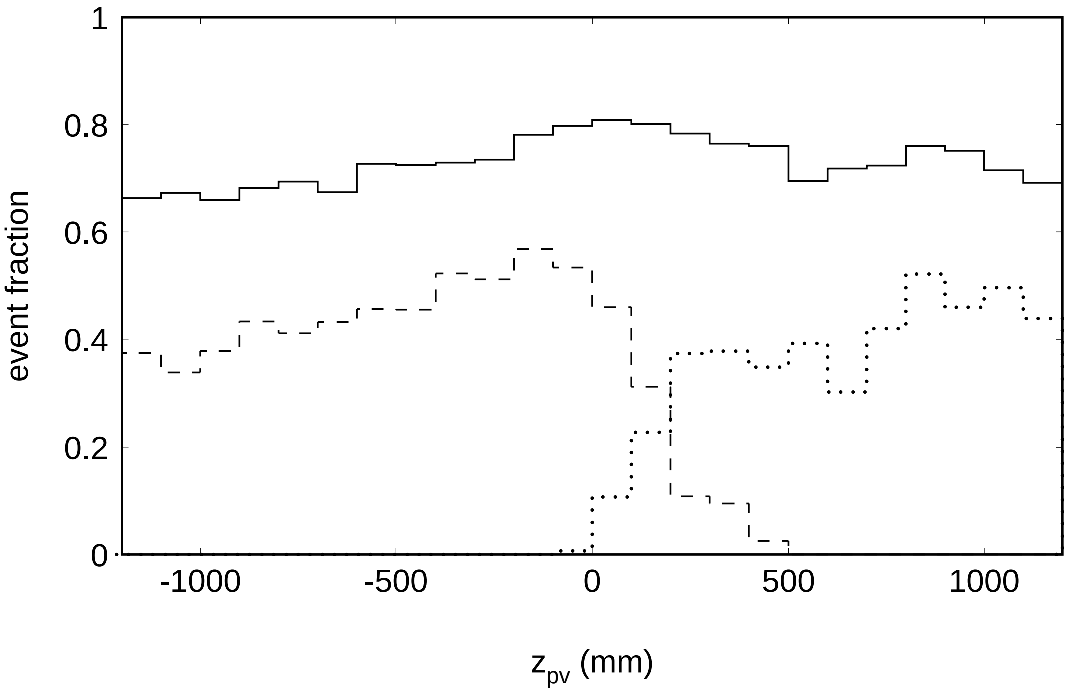

Fig. 2. Fraction of inelastic events with at least 6 reconstructable tracks as a function of the primary vertex position along the beam axis, for beam1-gas (dashed curve), beam2-gas (dotted curve) and beam-beam (solid curve) interactions at LHCb.

If we only retain interaction vertices that produce at least 6 reconstructable tracks, the average number of reconstructable tracks is about 9 for beam-gas interactions, while it is about 30 for beam-beam interactions and about 60 for beam-beam interactions that passed the LHCb trigger chain and produced a $b\bar{b}$ pair. Scaling with the square root of the number of tracks, one could expect for beam-gas interactions a primary vertex resolution [††] in x and y in the order of 30 μm, depending on the selection cuts. This should be compared with the expected beam sizes. For nominal LHC luminosity we expect at LHCb $\sigma_x \approx \sigma_y \approx 109$ μm, which is comfortably larger than the primary vertex resolution. For initial beam conditions, one might have smaller bunch charges ($N_1 = N_2 \approx 3 \times 10^{10}$ protons/bunch), hence $\sigma_x \approx \sigma_y \approx 32$ μm for the same luminosity, a value which is approaching the primary vertex resolution for beam-gas interactions. Clearly, the best way to carry out the proposed absolute luminosity measurement is to adapt the beam size at the interaction point (IP) to the available primary vertex resolution, such as to minimize systematic uncertainties associated with folding the vertex resolution and the

[††] Note that the vertex resolution might be somewhat better for beam1-gas than for beam2-gas interactions, since momentum information will be available for some of the tracks that pass through the LHCb trigger tracker and/or spectrometer.

distribution of interaction vertices. For the case of LHCb this would speak for a dedicated run with transverse beam sizes (σ_x, σ_y) of the order of 100-200 μm. As will be shown later, large beam sizes are also preferable for reducing possible sources of systematic uncertainties. Given the large rates expected for the LHC (both beams-gas and beam-beam rates), a few fills could be dedicated to the proposed method, using beam properties (charge, size, number of bunches, crossing angle, etc.) optimized for this calibration experiment.

4 Beam-gas and beam-beam events

Although measurements of the beam profiles with beam-gas interactions and of total bunch charges would be sufficient for an absolute luminosity determination, there is less interest in doing so if one cannot at the same time monitor a selected beam-beam collision process. The latter would allow pinning down a reference cross-section for all pp collision experiments at the same energy. Therefore, the simultaneous measurement of beam-gas and beam-beam interaction represents a great benefit, but also an additional challenge. We address this issue here.

At the LHC, in nominal running conditions, beam-beam effects are expected to be large. Due to the filling scheme, which contains gaps between bunch trains, some bunches will undergo less long-range collisions with counter-rotating bunches than others. In addition, certain bunches will endure different numbers of head-on collisions. In particular, some bunches do not collide at all at the LHCb IP. Simulations indicate that one can expect large variations of bunch shapes and positions due to beam-beam effects [15]. It is therefore beneficial to find *running conditions* for which these effects can be reduced and *selection cuts* that allow measuring simultaneously (i.e. for the same bunch) pA and pp collisions. The pros and cons of the various beam configurations are further discussed below. Here, we briefly investigate possible selection cuts.

Following on the numerical example given in section 2, Fig. 3 shows the distributions along the z axis of primary vertices with at least 6 reconstructable tracks. For this plot, 10 000 beam-gas inelastic events (for each beam) were generated flat in the range -1.2 m $< z_{pv} <$ 1.2 m, while 20 000 beam-beam inelastic events were generated assuming a Gaussian envelope centered on $z = 0$ and with rms $\sigma_z^{lum} = 53$ mm. The ratio of generated events corresponds to the conditions used for the rates given in expressions 5 and 6. As seen from Fig. 3, a simple cut on the primary vertex position (z_{pv}) would be sufficient to distinguish between the three types of events. One could e.g. request $z_{pv} < -5\sigma_z^{lum} \approx 265$ mm to select beam1-gas events, and $z_{pv} > 500$ mm to select beam2-gas events. Contamination by the other event samples (including beam-beam) would then be kept below 0.1%. To select beam-beam events

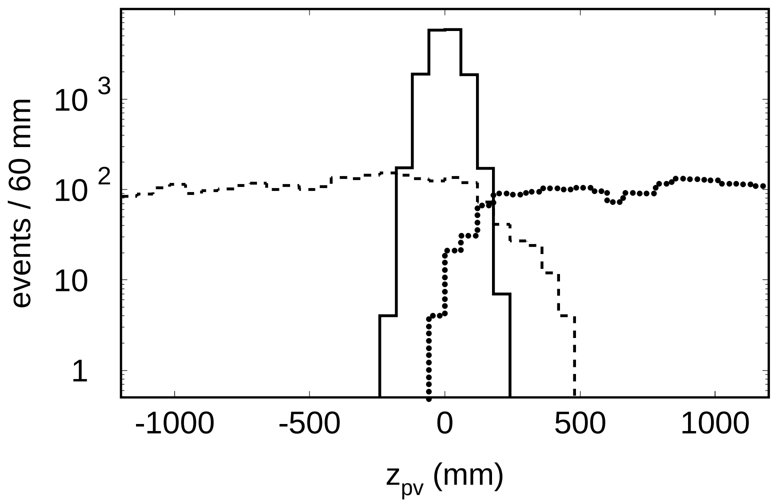

Fig. 3. Distributions along z of primary vertices with at least 6 reconstructable track for beam1-gas (dashed), beam2-gas (dotted) and beam-beam (solid) inelastic interactions. Beam-gas events were generated flat in the range -1.2 m $< z_{pv} <$ 1.2 m, while beam-beam events were generated assuming a Gaussian envelope with variance $\sigma_z^{lum} = 53$ mm.

one could request $|z_{pv}| < 2\sigma_z^{lum} \approx 106$ mm which reduces the beam-gas rates to the level of 3.5% while keeping more than 95% of the beam-beam events. Note that the exact distributions of each individual sample can be obtained from separate analysis of a pure beam-gas experiment (for either beam) and pure beam-beam experiments by running with gas but considering only non-colliding bunches (or running with a single beam in the ring) and, respectively, by running without target gas. This allows estimating precisely the contamination of a given sample by the other samples without relying on models or Monte-Carlo simulations.

To further distinguish the various events samples we consider the three following variables. In all cases, we show the distribution before applying any cut on z_{pv} and after applying the cuts $z_{pv} < -106$ mm, $|z_{pv}| < 106$ mm and $z_{pv} > 106$ mm:

- Fig. 4 shows the distributions of the number of reconstructable tracks. It is clearly seen that the number of tracks from the vertex allows further discrimination between beam-gas and beam-beam event samples.
- As is shown in Fig. 5, the highest p_T value among all the reconstructable tracks can also be used to distinguish between beam-gas and beam-beam events. Note however that, in the case of LHCb, a momentum measurement may not be obtained for tracks emerging from beam2-gas intertactions (the

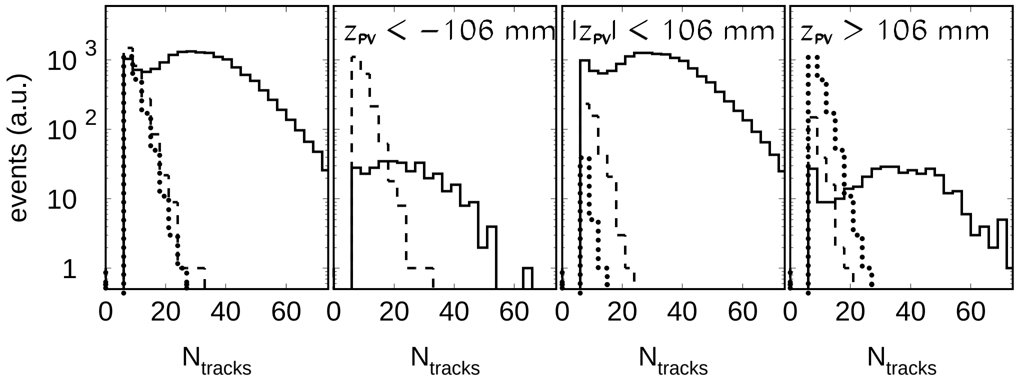

Fig. 4. Distributions of the number of reconstructable tracks (requiring at least 6). From left to right: no cut on z_{pv}, $z_{pv} < -106$ mm, $|z_{pv}| < 106$ mm, $z_{pv} > 106$ mm. Dashed curve: beam1-gas events; dotted curve: beam2-gas events; solid curve: beam-beam events.

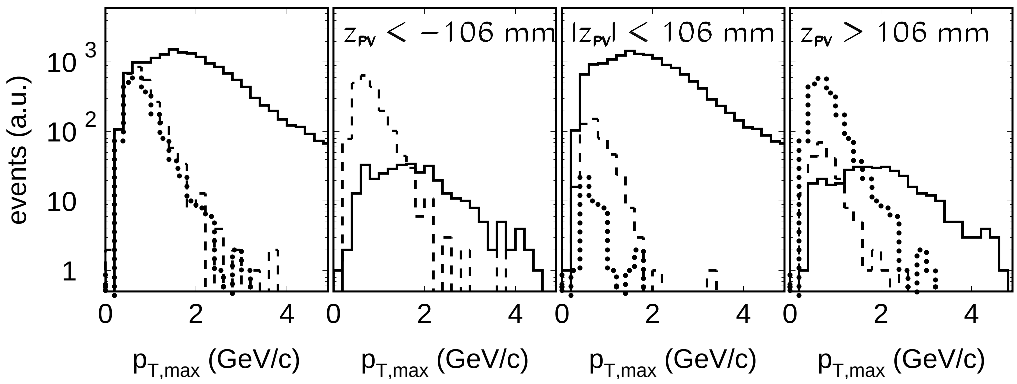

Fig. 5. Distributions of the highest p_T among all reconstructable tracks in the event (with at least 6 such tracks). From left to right: no cut on z_{pv}, $z_{pv} < -106$ mm, $|z_{pv}| < 106$ mm, $z_{pv} > 106$ mm. Dashed curve: beam1-gas events; dotted curve: beam2-gas events; solid curve: beam-beam events.

LHCb spectrometer acceptance is not symmetric, contrary to the ATLAS and CMS experiments).

- Fig. 6 shows the distributions of the average pseudo-rapidity of all reconstructable tracks emerging from the vertex. This allows distinguishing between beam-gas and beam-beam interactions, *and also* between beam1-gas and beam2-gas interactions.

If necessary, more sophisticated selection cuts can be found.

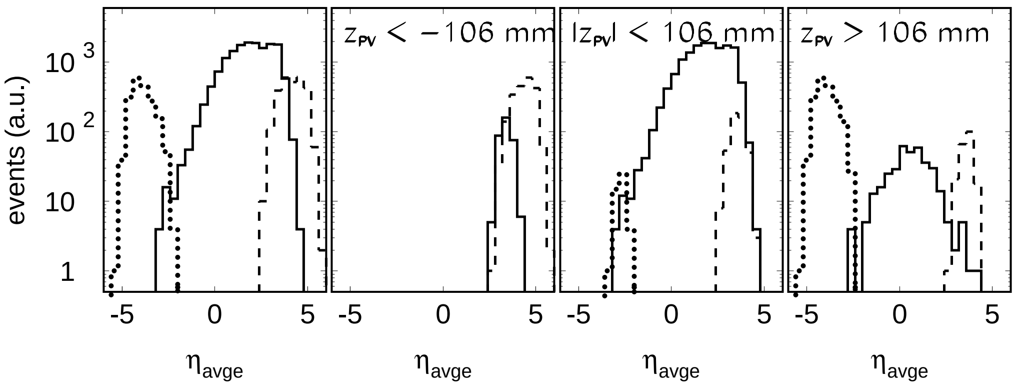

Fig. 6. Distributions of the average pseudo-rapidity of all reconstructable tracks coming from the vertex (requiring at least 6 tracks per vertex). From left to right: no cut on z_{pv}, $z_{pv} < -106$ mm, $|z_{pv}| < 106$ mm, $z_{pv} > 106$ mm. Dashed curve: beam1-gas events; dotted curve: beam2-gas events; solid curve: beam-beam events.

Inevitably, the reference cross-section for beam-beam collisions, which one is trying to determine with the method proposed in this work, will be measured over a reduced phase-space due to e.g. the finite detector acceptance, all possible detector efficiencies (trigger, reconstruction, etc.) and all cuts used in the data analysis of the event samples. This represents *no* limitation, as long as the same conditions and criteria are used to monitor, at a later stage, the absolute luminosity with the selected reference cross-section.

5 Potential sources of systematic uncertainties

We list here a number of effects which might give rise to systematic uncertainties and we propose ways to reduce these effects.

5.1 Beam-beam effects

Not all bunch pairs are necessarily giving the same overlap integral. Bunches undergo different numbers of head-on collisions and of long-range interactions. This gives them potentially different offsets at the IP and different shapes. As an example, for the LHC one expects beam offsets of the order of a few μm at IP1 (ATLAS) in nominal running conditions [15]. Therefore, the beam shapes and offsets obtained for given bunches from their interactions with gas should (a-priori) not be used to calculate the bunch overlap for other bunch pairs.

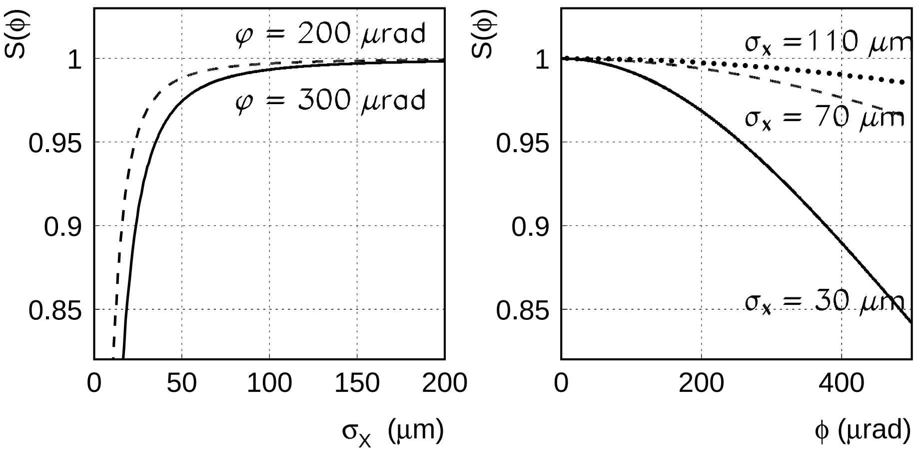

Fig. 7. Correction factor $S(\phi)$ for two different crossing angles ϕ as a function of the transverse beam size σ (left) and as a function of ϕ for different values of σ (right).

Transverse offsets will tend to reduce the luminosity, but such offsets can be measured precisely from beam-gas interactions. A longitudinal offset would be more difficult to measure, but would not affect the luminosity in first approximation (it would displace the IP and affect the luminosity via the 'hourglass effect', see below). Therefore, we see no serious limitations due to beam-beam effects. If unexpected systematic effects arise due to beam-beam effects, one can perform the proposed luminosity measurement with a reduced number of bunches, or even with a reduced bunch charge.

5.2 Crossing angle

In the presence of a crossing angle at the IP, the luminosity is reduced. In the simple case leading to expression 2, a correction factor must be introduced which depends on the beam crossing angle ϕ (the angle between the beam velocities $\mathbf{v}_1$ and $-\mathbf{v}_2$ is assumed here to be in the x-z plane). Expression 2 should be replaced by [11]

$$L = f \frac{N_1 \, N_2}{4\pi \, \sigma_x \, \sigma_y} S(\phi) \qquad \text{with } S(\phi) = \Big(1 + (\frac{\sigma_z}{\sigma_x} \tan\frac{\phi}{2})^2\Big)^{-1/2} . \tag{7}$$

The angle ϕ can be measured from beam-gas interactions of both beams. The uncertainty on this angle measurement will propagate into an uncertainty of the beam overlap integral. The correction factor $S(\phi)$ is shown in Fig. 7 for various values of the angle ϕ and of the transverse beam size σ_x. One sees that less sensitivity to the correction factor is obtained for larger beam sizes

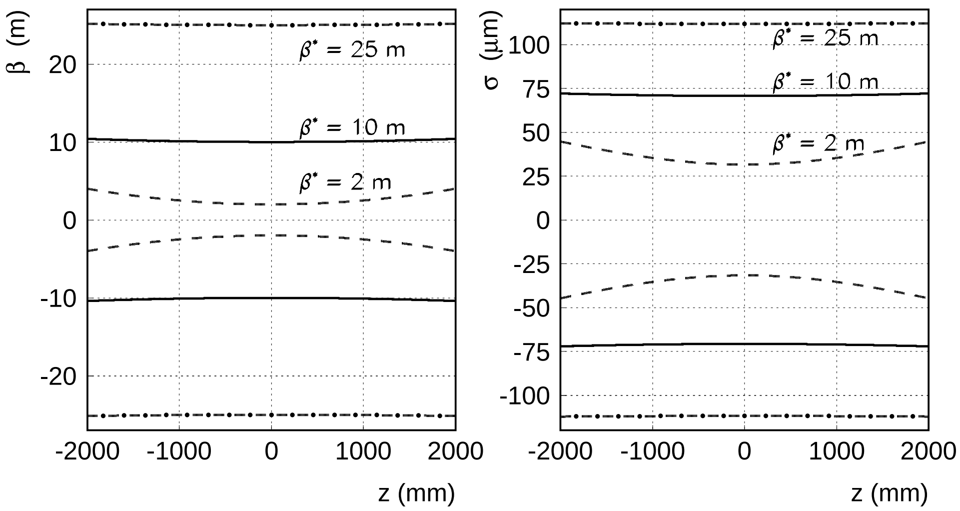

Fig. 8. Left: beta function $\beta(z)$ versus distance z from the IP for 3 values of β^*. Right: corresponding bunch rms $\sigma = \sqrt{\beta(z)\,\epsilon}$, using $\epsilon = 0.5$ nm.

and smaller angles. For example, at the LHC, with $\sigma_x > 100$ μm and crossing angles $\phi < 380$ μrad the correction factor stays between 0.99 and 1. Given a certain precision on the angle ϕ, one could choose an adequate β^* such that associated systematic uncertainties are kept to an acceptable level.

5.3 Varying beta function ('Hourglass effect')

The beta-function depends on the distance from the IP, which means that the bunch sizes vary (increase) as this distance increases. One expects approximately [11]

$$\beta(z) = [1 + (\frac{z}{\beta^*})^2]\,\beta^* \,. \tag{8}$$

This function is shown in Fig. 8 for typical values of β^* at IP8 of the LHC and for distances corresponding roughly to the z acceptance of the vertex detector considered in this work. One observes that for large β^* the variations of the beam size σ along z may well be negligible for $-2 < z < 2$ m, while these variations must clearly be taken into account for $\beta^* = 2$ m. Furthermore, such transverse beam size variations along z can be measured from beam-gas interaction data, even in the case of a varying gas density along the beam axis.

5.4 *Total bunch charge*

In the measurement of the luminosity, it is assumed that one can obtain by some means a measure of the bunch charges. These are the quantities N_1 and N_2 entering expression 1. One must pay attention that the values obtained, e.g. by measurements with fast current monitors, do correspond to the charges involved in the experiment at the IP. For example, at the LHC, 'ghost' bunches (or 'satellite' bunches) could occur every 2.5 ns. These contribute to the average current, but not necessarily to the measurable rate at the experiment. It is therefore important to measure not only the total beam current, but also the time structure of the beam charge. For the LHC, a relative accuracy of better than 1% (5%) is expected for nominal (pilot) bunches [16]. Inversely, satellite bunches that are not 'in time' may still contribute to the beam-beam luminosity. A small (satellite) bunch displaced by 2.5 ns may collide with a main bunch at 37.5 cm from the nominal IP and with another satellite bunch at the IP, etc. This could be determined from the data by looking at the shape of the luminous region for beam-beam events. One may also be able to identify bunches in the beam that are surrounded by less intense satellite bunches than others. Since the luminosity method proposed here applies for individual bunch pairs, one could study satellite-bunch systematic effects by comparing the results obtained with different bunch pairs.

5.5 *Transverse gas density inhomogeneities*

The method proposed in this paper to measure the absolute luminosity relies on the assumption of a known gas density profile in the transverse directions. In practice, we believe the gas density could be simply assumed to be constant in x and y. We check here that the ionization process does not deplete the gas density in the beam region for the case of the LHC. The ionization cross-section can be estimated from Ref. [17]. For 7 TeV protons crossing xenon gas we find approximately $\sigma_{\text{ioniz}} = 3.8 \times 10^{-18}$ cm^2. The average time spent in the beam region, when the atom does cross the beam region, is of order $t_{\text{on-beam}} \approx \sigma/v$ with $v = 2\sqrt{2k_B T/(\pi M_{\text{Xe}})} \approx 220$ m/s being the average velocity of xenon atoms with mass M_{Xe} at a temperature $T = 293$ K (k_B is Boltzmann's constant). Therefore, assuming $\sigma = 200$ μm, $t_{\text{on-beam}}$ is of the order of 1 μs. The probability P that this atom be ionized and kicked off by the bunch RF field during the time $t_{\text{on-beam}}$ is approximately given by

$$P = \frac{\sigma_{\text{ioniz}} N}{4\pi\sigma^2} \frac{t_{\text{on-beam}}}{t_{bb}} = \frac{\sigma_{\text{ioniz}} N}{4\pi\sigma\, v\, t_{bb}} \,. \tag{9}$$

For $N = 10^{11}$ and $t_{bb} = 25$ ns one gets $P \approx 3 \times 10^{-3}$.

Due to the fact that a zero crossing angle seems advantageous, for the reasons given in section 5.2, a large bunch spacing should be used for the proposed luminosity measurement at the LHC. Hence, we do not expect any measurable depletion of the gas density in the beam area, provided the time between bunches is kept large enough. Furthermore, the bunch-to-bunch gap may be used as a handle to study and/or remove possible 'hole-burning' effects.

5.6 Time variations

Time variations of the bunch parameters may introduce systematic uncertainties. Such variations are expected to increase with luminosity. At the LHC, in nominal conditions the beam decay rate is expected to be dominated by losses in head-on collisions, with a characteristic time of about 28 hours. This time is large compared to the time required to accumulate sufficient statistics for the measurement proposed in this work. One could reduce the beam losses even further to the limit that the beam decay time would be dominated by residual gas interactions (expected to be about 84 hours for the LHC). This would provide more stable (or slowlier varying) beam conditions during accumulation of beam-gas and beam-beam data for the luminosity measurement.

6 Experimental aspects

We gave in section 2 a numerical example assuming a certain pressure of noble gas (Xe). We discuss a little further some experimental aspects related to the gas target density, in particular for the case of the LHCb vertex detector [14].

The pumping speed for a noble gas like Xe in the VELO vacuum vessel is expected to be of the order of $C = 200$ ℓ/s using two ion pumps. Therefore, in order to achieve a residual gas pressure of about $p = 10^{-7}$ mbar, one would have to inject a gas flow of the order of $Q = 2 \times 10^{-5}$ mbar ℓ/s or 5×10^{14} Xe-atoms/s (at 293 K). If needed, the flow rate could be reduced in various ways, while keeping the useful gas target thickness constant. For instance, gas could be injected in a volume with small transverse dimensions encircling the beams [‡‡], taking advantage of the compression factor due to the small geometrical conductance for escaping the central volume. Optionally, one could reduce the pumping speed in the neighborhood of the IP. Assuming that a flow conductance of the order of 10 ℓ/s could be achieved, then the required throughput would be of the order of $Q = 10^{-6}$ mbar ℓ/s for a pressure of 10^{-7} mbar.

[‡‡] Such a geometry is already existing in the case of the VELO, see Ref. [14].

When carrying out the proposed luminosity measurement, one may be interested in comparing the measured pA and pp rates with gas injection 'on' and with gas injection 'off'. In this case a relevant quantity is the time constant τ_p involved in achieving a stable pressure. This time constant is given by $\tau_p = V/C$, where V is the volume of the vacuum vessel (beam vacuum). For the VELO one would have $V \approx 1000$ ℓ, or $\tau \approx 5$ s which is considerably smaller than the time constants involved in the beam and luminosity decay (~ 100 hours, see section 5.6). One could therefore consider alternating rapidly between 'gas on' and 'gas off', which would provide an additional handle to disentangle bunch-bunch events from bunch-gas events.

7 Summary

We have proposed a novel method to measure the absolute luminosity in colliding-beam experiments at circular accelerators. The method relies on reconstruction of vertices from beam-gas interactions to measure the colliding bunch profiles and to determine the beam overlap integral. The bunch charges are obtained separately from fast beam current monitors. If carefully implemented, this novel method might allow for measurements of the absolute luminosity with an accuracy of 1% or better. A dedicated running time of the order of one day at the LHC should be sufficient to carry out such an absolute luminosity measurement. Furthermore, when monitoring simultaneously the beam-gas rates and beam-beam rates for individual bunch pairs, this method should allow normalizing the cross-section of the selected beam-beam collisions with a precision not limited by statistics. This cross-section could then be used to determine the absolute luminosity during physics operation. For the LHC, we argued that smaller systematic uncertainties could be obtained when operating with sufficiently large beam size and no crossing angle (combined with an adequate bunch spacing). Clearly, all beam parameters can be controlled and should be varied to study possible systematic effects.

Acknowledgements

We are grateful to Werner Herr (CERN) and Noël Hilleret (CERN) for useful discussions on beam-beam effects and LHC vacuum, respectively. We would like to thank our LHCb collaborators for their comments and encouragement to publish this work.

References

[1] *"ATLAS Technical Proposal"*, CERN/LHCC/94-43, LHCC/P2, 15 December

1994.

[2] *"CMS Technical Proposal"*, CERN/LHCC/94-38, LHCC/P1, 15 December 1994.

[3] For a review, see for example *"Requirements from Precision Physics at LHC on the Luminosity Accuracy"*, S. Tapprogge in *"Forward Physics and Luminosity Determination at LHC"*, editors K. Huitu, V. Khoze, R. Orava, S. Tapprogge (World Scientific Publishing, 2001), and references therein.

[4] For an example see C. Augier et al., Phys. Lett. B **344**, 451 (1993).

[5] N. N. Khuri and T. Kinoshita Phys. Rev. **137**, B720 (1965).

[6] V. M. Budnev, I. F. Ginzburg, G. V. Meledin and V. G. Serbo, Nucl. Phys. B **63**, 519 (1973).

[7] M. Dittmar, F. Pauss, and D. Zürcher, Phys. Rev. D **56**, 7284 (1997).

[8] *"Calibration of the effective beam height in the ISR"*, S. van der Meer, ISR-PO/68-31, 1968 (CERN).

[9] See e.g. in J. Bosser et al., Nucl. Instrum. Methods A **235**, 475 (1985), P. Elmfors et al., Nucl. Instrum. Methods A **396**, 13 (1997), and *"LHC beam instrumentation conceptual design report"*, J. Bosser et al., LHC Project Report 370, 2000 (CERN).

[10] C. Møller, K. Dan. Vidensk. Selsk., Mat. Fys. Medd. **23**, 1 (1945).

[11] O. Napoly, Part. Acc. **40**, 180 (1993). See also in *"Concept of Luminosity"*, W. Herr and B. Muratori, Proceedings of the CERN Accelerator School, 2003 (in print).

[12] *"LHCb Reoptimized Detector Design and Performance Technical Design Report"*, R. Antunes Nobrega *et al.*, CERN/LHCC 2003-030, LHCb TDR 9, 9 September 2003.

[13] T. Sjostrand, P. Eden, C. Friberg, L. Lonnblad, G. Miu, S. Mrenna and E. Norrbin, Computer Physics Commun. **135**, 238 (2001).

[14] *"LHCb VELO Technical Design Report"*, P.R. Barbosa Marinho *et al.*, CERN/LHCC 2001-011, LHCb TDR 5, 31 May 2001. See also in Ref. [12].

[15] *"Features and implications of different LHC crossing schemes"*, W. Herr, LHC Project Report 628, 2003 (CERN); *"Effect of missing head-on collision on beam-beam effects in the LHC"*, W. Herr, LHC Project Note 321, 2003 (CERN); *"Effect of PACMAN bunches in the LHC"*, W. Herr, LHC Project Report 39, 1996 (CERN). See also in *"Beam-beam interactions"*, W. Herr, Proceedings of the CERN Accelerator School, 2003 (in print).

[16] See chapter 13 in *"LHC Design Report"*, vol. 1, *"The LHC Main Ring"*, CERN 2004-003-v1.

[17] F. F. Rieke and W. Prepejchal, Phys. Rev. A **6**, 1507 (1972).